Simple and reliable finite fault solutions for large earthquakes using the W-phase: The Maule (M_W = 8.8) and Tohoku (M_W = 9.0) earthquakes

Roberto Benavente[1] and Phil R. Cummins[1]

Received 6 May 2013; revised 5 June 2013; accepted 10 June 2013; published 22 July 2013.

[1] We explore the ability of W-phase waveform inversions to recover a first-order coseismic slip distribution for large earthquakes. To date, W-phase inversions for point sources provide fast and accurate moment tensor solutions for moderate to large events. We have applied W-phase finite fault inversion to seismic waveforms recorded following the 2010 Maule earthquake (M_w = 8.8) and the 2011 Tohoku earthquake (M_w = 9.0). Firstly, a W-phase point source inversion was performed to assist us in selecting the data for the finite fault solution. Then, we use a simple linear multiple-time-window method accounting for changes in the rupture velocity with smoothing and moment minimization constraints to infer slip and rake variations over the fault. Our results describe well the main features of the slip pattern previously found for both events. This suggests that fast slip inversions may be carried out relying purely on W-phase records. **Citation:** Benavente, R., and P. Cummins (2013), Simple and reliable finite fault solutions for large earthquakes using the W-phase: The Maule (M_w = 8.8) and Tohoku (M_w = 9.0) earthquakes, *Geophys. Res. Lett.*, *40*, 3591–3595, doi:10.1002/grl.50648.

1. Introduction

[2] Details of earthquake sources, such as fault orientation and the spatial variation of slip, are potentially useful in the first phases of disaster response. Understanding the proximity of fault rupture to population centers can be important for rapid casualty estimates [*Jaiswal and Wald*, 2011]. Understanding the spatial distribution of slip is especially important for large megathrust earthquakes, since tsunamigenicity is very sensitive to the amount of slip concentrated at shallow depth [*Satake and Tanioka*, 1999; *Hill et al.*, 2012]. These considerations have motivated recent work on the use of GPS data to estimate earthquake slip distributions in near real time [*Ohta et al.*, 2012; *Crowell et al.*, 2012]. These studies have demonstrated that dense GPS networks deployed in the near field of large earthquakes are able to obtain reliable estimates of slip distribution within minutes of an earthquake's occurrence, and are not prone to clipping, which plagues seismometer recordings in the near field.

[3] However, because not all megathrust earthquakes occur adjacent to dense GPS networks providing near real-time positioning, it is important to consider alternative means of obtaining rapid and reliable earthquake slip distributions. Seismic waves have long been used in finite fault inversions to obtain slip distributions for large earthquakes [see, e.g., *Hartzell and Heaton*, 1983], and several studies have considered the rapid application of such techniques [*Mendoza and Hartzell*, 2013; *Mendoza*, 1996; *Ammon et al.*, 2006; *Dreger et al.*, 2005]. These studies either use regional seismic waveforms or teleseismic body and surface waves. However, these methods often require sophisticated processing and manual review and can be sensitive to 3-D earth structure. Here, we consider use of the W-phase [*Kanamori*, 1993] in finite fault inversion as an alternative that can potentially overcome some of the difficulties with using seismic body and surface waves in rapid finite fault inversions.

[4] The W-phase has gained special importance as a technique for point source inversions for large earthquakes. First reported by *Kanamori* [1993], the W-phase is a long period wave arriving at the recording station together with the *P* wave. Because of its small amplitude and the time window used (prior to *S* wave arrivals), the inversion of W-phase waveforms provides an effective method for rapid determination of the moment tensor. Moreover, if the instrument response is deconvolved in the time domain, the clipping in the records typical for large events can be avoided. Thus far, W-phase inversion has been shown to be a robust and reliable method for point source inversion for large earthquakes $M_w > 6.5$ [*Kanamori and Rivera*, 2008; *Duputel et al.*, 2012a], and it is a standard solution in the U.S. Geological Survey (USGS) catalog. In addition, multiple-point-source inversions of W-phase waveforms were introduced by *Duputel et al.* [2012b] in order to explain the source complexity of the 2012 Sumatra great strike-slip event (Mw = 8.6). These characteristics have led us to evaluate the use of the W-phase in the slip distribution problem.

[5] To recover the coseismic slip, different types of data can be used (geodetic, teleseismic, tsunami records, etc.), although far field seismic records play an important role because they are widely available within minutes after an earthquake occurs. The use of teleseismic data to constrain the spatial slip distribution was introduced by *Hartzell and Heaton* [1983]. They considered a predetermined fault plane divided into a number of subfaults and solved for their moment using constant rupture velocity. While many improvements have been made to this approach (a review can be found in *Ide* [2007]), the philosophy of the most recent methods remains similar: Discretize the source's

Additional supporting information may be found in the online version of this article.

This article was originally published on line on 22 July 2013. Revised supporting information was supplied, and the article was reposted on 1 August 2013.

[1]Research School of Earth Sciences, Australian National University, Canberra, ACT, Australia.

Corresponding author: R. Benavente, Research School of Earth Sciences, Australian National University, Canberra, ACT 0200, Australia. (roberto.benavente@anu.edu.au)

0094-8276/13/10.1002/grl.50648

surface into a number of units that can be treated as point sources. A simultaneous inversion is then carried out for the moment of each unit. Then, the spatial and temporal distribution of the slip for the whole fault is recovered by mapping the point source solutions in the fault plane.

[6] In this study, we consider the utility of the W-phase to extract information about the finite character of faulting in major earthquakes. To this end, we applied a finite slip inversion for two recent large megathrust earthquakes: the 2010 Maule (M_w = 8.8) and the 2011 Tohoku (M_w = 9.0). Both of them excited devastating tsunami waves and have numerous finite fault solutions available [e.g., *Lay et al.*, 2010; *Wang et al.*, 2012; *Koper et al.*, 2012; *Ammon et al.*, 2011; *Lay et al.*, 2011]. The Maule earthquake occurred offshore central Chile. The W-phase point source solution (http://earthquake.usgs.gov/earthquakes/eqinthenews/2010/us2010tfan/neic_tfan_wmt.php), hereafter referred to as WPPS, yields a moment of $M_0 = 2.0 \cdot 10^{22}$ Nm, a fault plane with strike γ = 16° and dip δ = 14°, and a rake angle of λ = 104°; for a centroid located at 35.83°S, 72.67°W and depth 35 km using 28 stations. For the Tohoku earthquake WPPS is reported in detail by *Duputel et al.* [2011]. They found a total moment of $M_0 = 4.26 \cdot 10^{22}$ Nm, a fault plane with γ = 196° and δ = 12°, and λ = 85°; for a centroid located at 37.92°N, 143.11°E and depth 19.5 km using 69 stations. In both earthquakes, WPPS agrees fairly well with the standard Global Centroid Moment Tensor (GCMT) and USGS solutions.

2. Inversion Procedure

[7] As usual in the finite source inversions, the first step in our procedure is the data selection. Because of the large number of parameters involved in the inversion, it is crucial to identify and remove corrupt data (e.g., dead channels and wrong instrument response information) prior to the inversion. To address this issue, we first perform a point source inversion, following *Kanamori and Rivera* [2008]. W-phase inversion can be performed using the three displacement components, but the horizontal components are often noisy in the W-phase frequency band. Indeed, after a rigorous noise analysis for the Tohoku event *Duputel et al.* [2011] reached a final low-noise data set composed mostly of vertical component waveforms. Thus, for both events, we retrieve LHZ channels for stations in a distance range of 5 – 90° from the epicenter. We take the centroid's location, the half duration t_h and the time delay t_d from the WPPS in the USGS website for the Maule event and from *Duputel et al.* [2011] for the Tohoku event. We deconvolve the traces in the time domain and bandpass them using a Butterworth filter in the band 200–1000 s. After trimming the data in the typical W-phase time window (t_p, t_p + 15Δ, Δ: station-epicenter distance in degrees), we remove the stations presenting anomalous traces based on the median criterion described by *Duputel et al.* [2012a]. Next, we invert for the moment tensor components (Using the same database of Green Functions as *Kanamori and Rivera* [2008]). We reject all the traces with a high individual misfit, and a final inversion is performed.

[8] Apart from the data selection, it is necessary to set the subfault parameters. We carried out a number of synthetic checkerboard tests to find out the optimal subfault size that can be used in this approach. We found that subfaults as small as 15 km by 15 km can be resolved. Nevertheless, solutions are extremely unstable (i.e., sensitive to the noise) and therefore we favor a subfault size of 30 km by 30 km, which better tolerates the introduction of noise (see Figures S1 and S2 in the supporting information). We used the fault geometry provided by the point source solutions. In both earthquakes, the actual fault plane can be easily distinguished from the point source solution using the subduction geometry. In general, the WPPSs we obtain do not differ greatly from the USGS and GCMT solutions, and we achieve similar results using a fault geometry from any of them.

[9] A rupture velocity must be determined (or guessed) in order to invert for the moment of each subfault [*Hartzell and Heaton*, 1983; *Mendoza and Hartzell*, 1988]. We first used a simple source time function consisting of one triangle, and used a constant rupture velocity, but the results for the Tohoku event were not compatible with most of the finite slip solutions we are aware of. Examples of solutions we obtained using this approach can be found in Figure S3. After performing several inversions using different values of v_r, we found that for the Tohoku event, the best fit is in the range of 1.5–3 km/s, while for the Maule event 2–3 km/s is the best. In these ranges, the W-phase appears not to be extremely sensitive to the rupture velocity. Nevertheless, the results were symmetric patterns with two regions of concentrated slip far away from the hypocenter. For the Tohoku earthquake, this is in disagreement with most of the results in the literature that locate most of the slip above the hypocenter, near to the trench. These symmetric patterns appear to be a result of the an oversimplified rupture model [*Hartzell and Langer*, 1993]. Therefore, we prefer to include possible variations in the rupture velocity in our approach using a slightly more complex source time function.

[10] We adopt a fairly simple multi-time window method [e.g., *Olson and Apsel*, 1982; *Ide*, 2007] in order to account for variations in the rupture velocity. The maximum rupture velocity v_r^m is chosen in accordance with the values discussed in the literature for each event. For each subfault, we use a source time function composed of N_t triangles and half duration t_h depending on the event. The triangles are overlapped by the same amount t_h so each subfault is allowed to slip N_t times at successive time increments of t_h after a rupture front with velocity v_r^m reaches the subfault.

[11] Because of the bandpass filtering applied to the data, they are insensitive to variations in frequency content at periods less than 200 s, which is far longer than typical earthquake rise times. On the other hand, the phase shift associated with a delay of t_h, even when it is as small as the 10 and 15 s used for the Maule and Tohoku earthquakes, respectively, is detectable in the waveforms given the good signal-to-noise ratio that is typical in W-phase inversions. This sensitivity of the W-phase waveform inversions to phase shift is consistent with our tests using constant rupture velocity, as well as with the ability of the W-phase to resolve spatial variations in slip as indicated by our checkerboard resolution tests. In practice, this time shift enables the W-phase to distinguish variations in rupture velocity as well as spatial variations in cumulative slip.

[12] Finally, as usual in finite slip inversions, we impose smoothing and moment minimization constraints to deal with the typical instability arising from the overdetermined

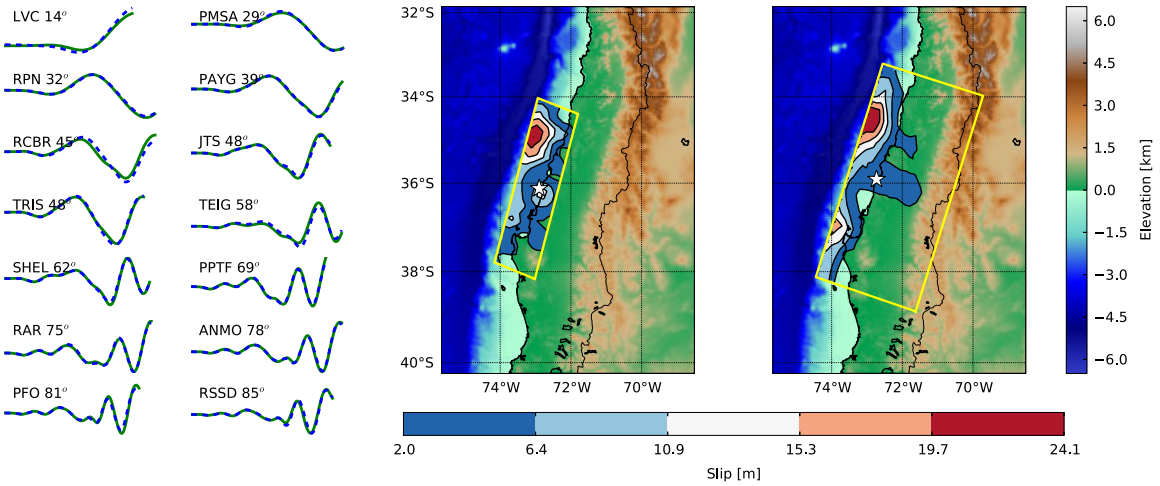

Figure 1. Results for the Maule event. (left) Waveform fits are shown for selected stations. Observed displacements and their respective synthetics are indicated by a continuous green line and a dashed blue line, respectively. Note that each trace is plotted in the W-phase time window (t_p, $t_p + 15\Delta$, Δ: station-epicenter distance in degrees) and the epicentral distance is shown next to the station name. (middle) A reference model is plotted from *Koper et al.* [2012]. Different slip regions are indicated by contours, the yellow rectangle marks the faulting area considered, and the hypocenter is indicated by a white star. (right) The achieved solution plotted in the same way as the reference model inf Figure 1 (middle).

matrices involved in the inversion problem. Requiring a solution to be smooth means that we prefer solutions in which the moment of two neighboring subfaults is similar. Minimizing the moment implies that subfaults which do not contribute much to the general fit must be forced to be zero. In both cases, the stabilization of the solution is achieved by appending a set equations to the original system. Therefore, our inversion problem has the following appearance:

$$\begin{bmatrix} \mathbf{A} \\ \lambda_1 \mathbf{I} \\ \lambda_2 \mathbf{F} \end{bmatrix} \cdot \mathbf{x} = \begin{bmatrix} \mathbf{B} \\ \mathbf{0} \\ \mathbf{0} \end{bmatrix}, \tag{1}$$

where **A** is a matrix with the synthetics of each subfault, **B** is a vector with the observed seismograms, **x** is a vector containing the unknown moment of each subfault, **I** is the identity matrix, **F** is a finite difference Laplacian operator applied over each time window, and λ_1 and λ_2 are the moment minimization and smoothing weights, respectively. These weights are determined such that the overall misfit of the solution does not increase greatly. In our parameter vector **x**, we include two elements for each subfault to account for variations in rake.

3. Results

[13] In this section, we present the results of applying our finite fault inversion approach to the Maule and Tohoku earthquakes. Typically, teleseismic finite fault inversion solutions differ from one to another, especially when they are computed soon after the event. Because of that, we are more interested in testing whether our solutions can reproduce roughly the spatial accumulated slip distribution rather than match every detail in a particular solution.

[14] It should also be noted that the results of the W-phase inversion are the seismic moments of the individual point sources comprising the finite fault solution, and the Green's functions used in the inversion are calculated using the preliminary reference Earth model (PREM) [*Dziewonski and Anderson*, 1981]. PREM is a good representation for globally averaged earth structure, which should be appropriate for the very long wavelengths associated with the W-phase. In order to compare our results with published finite fault models, we have converted seismic moment to slip, and in doing so, we have accounted for small-scale variations with depth of rigidity structure near the source by using local crustal velocity models instead of PREM.

3.1. Maule Earthquake

[15] In this event, we use 31 LHZ channels with a good azimuthal coverage. We base the 1-D rigidity structure at the source on the CRUST 2.0 averaged continental model (http://igppweb.ucsd.edu/~gabi/crust2.html). For v_r, t_h and N_t we choose 2.5 km/s, 10 s and 3, respectively. Strike ϕ, dip δ, and the initial guess of the rake λ are taken as 18°, 18°, and 104°, respectively. The hypocenter we use is located at 35.9°S, 72.7°W and depth 35 km. In Figure 1 (left), some of the traces of both observed and synthetic waveforms are shown. As is often the case in W-phase inversions, they match quite well [*Kanamori and Rivera*, 2008; *Duputel et al.*, 2012a] giving a percent misfit (L1 norm) of 12.1%, while our WPPS yields 16.3%. As one would expect, the higher number of parameters of the finite fault solution leads to a better fitting compared to WPPS.

[16] The cumulative slip distribution is shown in Figure 1 (right). Our solution exhibits some properties which are present in most published finite fault inversions of this earthquake: bilateral rupture with most significant slip concentrated northwest of the epicenter and little slip close to the epicenter (*Koper et al.* [2012]. This model is also included in Figure 1 at the center, for comparison). As pointed out by [*Vigny et al.*, 2011], a high slip close to the trench in this event might be supported by the great tsunami generated afterwards and the fact that a number of aftershocks have been located in this region. We find a total moment of $M_0 = 2.0 \cdot 10^{22}$ Nm. The rake angle (Figure S4, top) is

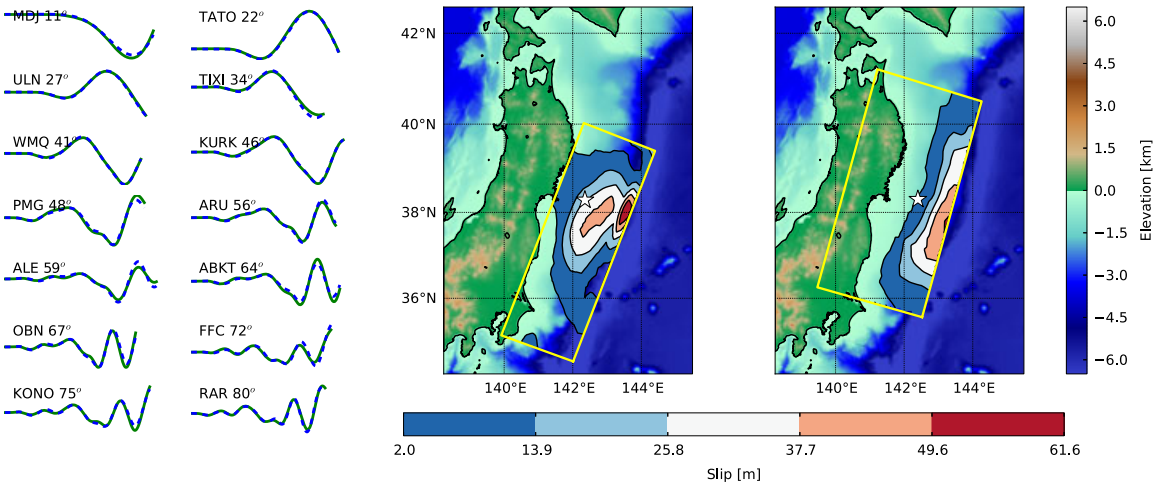

Figure 2. Results for the Tohoku event. The details are the same as Figure 1. However, in this case, the reference solution in Figure 2 (middle) is from *Ammon et al.* [2011]. The source rigidity structure we used for both the W-phase solution (Figure 2, right) and the reference solution is from *Lay et al.* [2011].

mostly dip-slip in the two regions in which the slip is mostly concentrated. Between these two regions, above the hypocentre, there is an area of small slip, mostly of strike-slip geometry.

3.2. Tohoku Earthquake

[17] The Tohoku earthquake was characterized using 65 LHZ channels. We employ the same rigidity structure described in *Lay et al.* [2011]. For that event we use $t_h = 15$ s, $v_{r^m} = 2.5$ km/s and $N_t = 4$. The last value attempts to describe the broader rupture velocity range for this event described in the literature. In fact, *Ammon et al.* [2011] using teleseismic *P* wave inversion found that a slow rupture propagation followed by a faster propagation was required for a satisfactory solution. In addition, backprojection analysis [*Koper et al.*, 2011; *Wang and Mori*, 2011] shows that after a slow rupture initiation (∼1.0 km/s), the rupture could reach up to 3 km/s. In this event, we locate the hypocenter at 38.3°N, 142.4°E, and depth 30 km based on the USGS solution (http://earthquake.usgs.gov/earthquakes/eqinthenews/2011/usc0001xgp/#details). The fault plane is defined by strike $\phi = 196°$ and $\delta = 12°$, and the initial rake is $\lambda = 85°$. The solution predicts the observations well as can be seen in Figure 2 (left), with a percent misfit (L1 norm) of 12.9%, as compared to our WPPS misfit of 15.9%.

[18] Figure 2 (right) presents the spatial distribution of the slip we obtained. Our result shows a rake of around 90° (see Figure S4, bottom) and concentrates the higher slip in the shallowest part of the fault, above the hypocenter. This feature can be found in most of the slip distributions calculated for this event [e.g., *Lay et al.*, 2011; *Hayes*, 2011]. For reference, in Figure 2 (center), we show the solution from *Ammon et al.* [2011] after including the rigidity structure from *Lay et al.* [2011], which we also use for our model. The maximum slip value is ∼60 m in the reference solution (Figure 2, center) and ∼50m in our model (Figure 2, right). While the exact value of the highest slip is hard to constrain in our approach, this general slip pattern turns out to be quite stable to variations of λ_1 and λ_2. Moreover, the moment we find with this model is $M_0 = 4.1 \cdot 10^{22}$ Nm which is in agreement with most of the values in the literature. Finally, as mentioned earlier, the misfit of this model is well below what we find in the point source solution.

4. Discussion

[19] We have performed a finite fault inversion of the 2010 Maule ($M_w = 8.8$) and the 2011 Tohoku ($M_w = 9.0$) earthquakes, using a data set consisting of W-phase waveforms, mostly from the Global Seismic Network. In both cases, our results for the cumulative coseismic slip show consistency with other models in the literature and can describe first-order characteristics of the rupture. We employ a multiple-time window method [*Olson and Apsel*, 1982] allowing for rupture velocity variations while keeping the problem linear. The simplicity of the resulting methodology and the accuracy of the results suggest that this method might be suitable to obtain preliminary rupture models in the case of large events. One problem would be, however, to rapidly determine or estimate all the parameters required in the inversion. Nevertheless, some of these critical parameters may be obtained using simple approaches. For instance, t_h may be related to the magnitude of the event as in point sources [*Duputel et al.*, 2012a], λ_1 and λ_2 can be computed with an empirical relation as has been proposed by *Mendoza and Hartzell* [2013] for finite fault inversion with *P* waves. The problem on how to determine the fault dimensions can be addressed using the method suggested by *Rivera et al.* [2012]. In the case of megathrust earthquakes, the best alternative to decide the faulting plane, as has been suggested by *Hayes et al.* [2011], may be to constrain it to the slab geometry. Finally, the sensitivity of this methodology to the use of different a priori rupture velocities needs to be explored, perhaps with a higher number of events.

[20] **Acknowledgments.** We thank L. Rivera, H. Kanamori, and Z. Duputel for providing us with Green Functions database we used in this research. The data acquisition and processing was done mostly using ObsPy. The reference solutions were supplied by T. Lay for the Maule earthquake and acquired from the C. Ammon website (http://eqseis.geosc.psu.edu/~cammon/Japan2011EQ/) for the Tohoku event. R. Benavente is supported by CONICYT, Chile, through its scholarships program "Becas Chile". This research was partially funded by Australian Research Grant DP110101983.

[21] The Editor thanks Victor Tsai and an anonymous reviewer for their assistance in evaluating this paper.

References

Ammon, C. J., A. A. Velasco, and T. Lay (2006), Rapid estimation of first-order rupture characteristics for large earthquakes using surface waves: 2004 Sumatra-Andaman earthquake, *Geophys. Res. Lett.*, *33*, L14314, doi:10.1029/2006GL026303.

Ammon, C. J., T. Lay, H. Kanamori, and M. Cleveland (2011), A rupture model of the 2011 off the Pacific coast of Tohoku Earthquake, *Earth Planets Space*, *63*(7), 693–696.

Crowell, B. W., Y. Bock, and D. Melgar (2012), Real-time inversion of GPS data for finite fault modeling and rapid hazard assessment, *Geophys. Res. Lett.*, *39*, L09305, doi:10.1029/2012GL051318.

Dreger, D. S., L. Gee, P. Lombard, M. H. Murray, and B. Romanowicz (2005), Rapid finite-source analysis and near-fault strong ground motions: Application to the 2003 Mw 6.5 San Simeon and 2004 Mw 6.0 Parkfield earthquakes, *Seismol. Res. Lett.*, *76*(1), 40–48.

Duputel, Z., L. Rivera, H. Kanamori, G. Hayes, B. Hirshorn, and S. Weinstein (2011), Real-time W phase inversion during the 2011 off the Pacific coast of Tohoku Earthquake, *Earth Planets Space*, *63*(7), 535–539.

Duputel, Z., L. Rivera, H. Kanamori, and G. Hayes (2012a), W phase source inversion for moderate to large earthquakes (1990–2010), *Geophys. J. Int.*, *189*(2), 1125–1147.

Duputel, Z., H. Kanamori, V. C. Tsai, L. Rivera, L. Meng, J.-P. Ampuero, and J. M. Stock (2012b), The 2012 Sumatra great earthquake sequence, *Earth Planet. Sci. Lett.*, *351*, 247–257.

Dziewonski, A. M., and D. L. Anderson (1981), Preliminary reference earth model (PREM), *Phys. Earth Planet. Inter.*, *25*, 297–356.

Hartzell, S., and T. Heaton (1983), Inversion of strong ground motion and teleseismic waveform data for the fault rupture history of the 1979 Imperial Valley, California, earthquake, *Bull. Seismol. Soc. Am.*, *73*(6A), 1553–1583.

Hartzell, S., and C. Langer (1993), Importance of model parameterization in finite fault inversions: Application to the 1974 Mw 8.0 Peru earthquake, *J. Geophys Res.*, *98*, 22,123–22,134.

Hayes, G. P. (2011), Rapid source characterization of the 2011 Mw 9.0 off the Pacific coast of Tohoku earthquake, *Earth Planets Space*, *63*(7), 529–534.

Hayes, G. P., et al. (2011), 88 Hours: The US Geological Survey National Earthquake Information Center Response to the 11 March 2011 Mw 9.0 Tohoku Earthquake, *Seismol. Res. Lett.*, *82*(4), 481–493.

Hill, E. M., et al. (2012), The 2010 Mw 7.8 Mentawai earthquake: Very shallow source of a rare tsunami earthquake determined from tsunami field survey and near-field GPS data, *J. Geophys. Res.*, *117*, B06402, doi:10.1029/2012JB009159.

Ide, S. (2007), Slip inversion, in *Treatise On Geophysics*, vol. 4, edited by H. Kanamori, Elsevier, Amsterdam.

Jaiswal, K., and D. Wald (2011), Rapid estimation of the economic consequences of global earthquakes, *U.S. Geol. Surv. Open File Rep., 2011-1116*.

Kanamori, H. (1993), W Phase, *Geophys. Res. Lett.*, *20*(16), 1691–1694.

Kanamori, H., and L. Rivera (2008), Source inversion of W phase: Speeding up seismic tsunami warning, *Geophys. J. Int.*, *175*(1), 222–238.

Koper, K. D., A. R. Hutko, T. Lay, C. J. Ammon, and H. Kanamori (2011), Frequency-dependent rupture process of the 2011 Mw 9.0 Tohoku Earthquake: Comparison of short-period P wave backprojection images and broadband seismic rupture models, *Earth Planets Space*, *63*(7), 599-602.

Koper, K. D., A. R. Hutko, T. Lay, and O. Sufri (2012), Imaging short-period seismic radiation from the 27 February 2010 Chile (Mw 8.8) earthquake by back-projection of P, PP, and PKIKP waves, *J. Geophys. Res.*, *117*, B02308, doi:10.1029/2011JB008576.

Lay, T., C. Ammon, H. Kanamori, K. Koper, O. Sufri, and A. Hutko (2010), Teleseismic inversion for rupture process of the 27 February 2010 Chile (Mw 8.8) earthquake, *Geophys. Res. Lett.*, *37*, L13301, doi:10.1029/2010GL043379.

Lay, T., C. J. Ammon, H. Kanamori, L. Xue, and M. J. Kim (2011), Possible large near-trench slip during the 2011 Mw 9.0 off the Pacific coast of Tohoku Earthquake, *Earth Planets Space*, *63*(7), 687–692.

Mendoza, C. (1996), Rapid derivation of rupture history for large earthquakes, *Seismol. Res. Lett.*, *67*(6), 19–26.

Mendoza, C., and S. Hartzell (2013), Finite-fault source inversion using teleseismic P waves: Simple parameterization and rapid analysis, *Bull. Seismol. Soc. Am.*, *103*(2A), 834–844.

Mendoza, C., and S. H. Hartzell (1988), Inversion for slip distribution using teleseismic P waveforms: North Palm Springs, Borah Peak, and Michoacan earthquakes, *Bull. Seismol. Soc. Am.*, *78*(3), 1092–1111.

Ohta, Y., et al. (2012), Quasi real-time fault model estimation for near-field tsunami forecasting based on RTK-GPS analysis: Application to the 2011 Tohoku-Oki earthquake (Mw 9.0), *J. Geophys. Res.*, *117*, B02311, doi:10.1029/2011JB008750.

Olson, A. H., and R. J. Apsel (1982), Finite faults and inverse theory with applications to the 1979 Imperial Valley earthquake, *Bull. Seismol. Soc. Am.*, *72*(6A), 1969–2001.

Rivera, L., Z. Duputel, and H. Kanamori (2012), Toward rapid determination of the source finiteness of large earthquakes, Abstract S43H-02 presented at 2012 Fall Meeting, AGU, San Francisco, Calif.

Satake, K., and Y. Tanioka (1999), Sources of tsunami and tsunamigenic earthquakes in subduction zones, *Pure Appl. Geophys.*, *154*, 467–483.

Vigny, C., et al. (2011), The 2010 Mw 8.8 Maule megathrust earthquake of Central Chile, monitored by GPS, *Science*, *332*(6036), 1417–1421.

Wang, D., and J. Mori (2011), Rupture process of the 2011 off the Pacific coast of Tohoku Earthquake (Mw 9.0) as imaged with back-projection of teleseismic P-waves, *Earth Planets Space*, *63*(7), 603–607.

Wang, L., C. Shum, F. Simons, A. Tassara, K. Erkan, C. Jekeli, A. Braun, C. Kuo, H. Lee, and D. Yuan (2012), Coseismic slip of the 2010 Mw 8.8 Great Maule, Chile, earthquake quantified by the inversion of GRACE observations, *Earth Planet. Sci. Lett.*, *335*, 167–179.